

# Effect of Carbon Dioxide Sorption on the Phase Behavior of Weakly Interacting Polymer Mixtures: Solvent-Induced Segregation in Deuterated Polybutadiene/Polyisoprene Blends

VIJAYAKUMAR S. RAMACHANDRARAO, BRYAN D. VOGT, RAVI R. GUPTA, JAMES J. WATKINS

Department of Chemical Engineering, University of Massachusetts, Amherst, Massachusetts 01003

Received 5 February 2003; revised 8 July 2003; accepted 19 July 2003

**ABSTRACT:** The effect of carbon dioxide (CO<sub>2</sub>) sorption on the lower critical solution temperatures of deuterated polybutadiene/polyisoprene blends was determined with *in situ* small-angle neutron scattering. CO<sub>2</sub> was a poor solvent for both polymers and exhibited very weak selectivity between the blend components. The sorption of modest concentrations of CO<sub>2</sub>, at pressures up to 160 bar, induced phase segregation at temperatures well below the binary-phase-separation temperature and caused an increased asymmetry in the lower critical solution temperature curve. The origin of solvent-induced phase segregation in this weakly interacting polymer blend system was attributed predominantly to an exacerbation of the existing disparity in the compressibility of the components upon CO<sub>2</sub> sorption. © 2003 Wiley Periodicals, Inc. *J Polym Sci Part B: Polym Phys* 41: 3114–3126, 2003

## INTRODUCTION

We are investigating the effect of compressible fluid sorption on the phase behavior of block copolymers and blends.<sup>1–5</sup> Results to date indicate that for systems that exhibit upper critical solution behavior, the sorption of carbon dioxide (CO<sub>2</sub>) or light alkanes promotes miscibility.<sup>2,3,6</sup> For light alkane solvents, the depth of the depression scales with the volume fraction of the sorbed diluent, regardless of the alkane chain length.<sup>3</sup> These results are consistent with those expected from liquid solvents and, as discussed later, arise predominantly from the screening of unfavorable segmental interactions between the blocks.

The analogy between the effects of liquid and compressible diluents, however, breaks down for the phase behavior in systems exhibiting lower

critical solution behavior. Recently, we reported dramatic depressions of the lower critical solution temperatures (LCSTs) of polymer mixtures, including polystyrene (PS)/poly(vinyl methyl ether) (PVME) and deuterated polystyrene (d-PS)/poly(*n*-butyl methacrylate) (PnBMA) blends.<sup>1,4</sup> Depressions in the lower disorder–order transitions (LDOTs) of over 250 °C for the diblock copolymer system poly(styrene-*b*-*n*-butyl methacrylate) [P(S-*b*-nBMA)] upon the sorption of small amounts of CO<sub>2</sub> or light alkanes were also observed.<sup>1,4</sup> Moreover, for a series of light alkanes, the depth of the depression of the LDOT of P(S-*b*-nBMA) upon fluid sorption does not scale universally with the sorbed volume fraction, as in the case of the order–disorder transition (ODT) system [poly(styrene-*b*-isoprene), P(S-*b*-I)]. Rather, the depression is most severe for the most compressible solvent, methane, and is progressively less dramatic for ethane, propane, and butane.<sup>3</sup> By contrast, the dilution of P(S-*b*-nBMA) with tetradecane, a saturated liquid alkane, increases the LDOT.

Correspondence to: J. J. Watkins (E-mail: watkins@ecs.umass.edu)

*Journal of Polymer Science: Part B: Polymer Physics*, Vol. 41, 3114–3126 (2003)  
© 2003 Wiley Periodicals, Inc.

The fact that compressible fluid sorption promotes miscibility in upper critical solution temperature (UCST)-type systems and can induce phase segregation in LCST-type systems is likely attributable to both the underlying nature of these transitions and the consequences of compressed fluid sorption in polymers. UCST-type transitions, including ODTs, are enthalpically driven, and phase separation occurs with cooling because of unfavorable interactions between polymer segments. By comparison, in the absence of strong specific interactions between the segments, phase separation upon heating at the LCST or LDOT is driven by entropic considerations, namely, equation-of-state (EOS) effects that arise because of the disparities in component compressibilities.<sup>7–10</sup> Such disparities can impose unfavorable volume changes on mixing that destabilize the system.<sup>11</sup>

The sorption of compressible fluids can influence the location of these transitions in several ways. First, the sorbed diluent can screen unfavorable polymer–polymer interactions, an enthalpic contribution that can promote miscibility in blends and block copolymers. However, the fluid (CO<sub>2</sub> or a light alkane) is generally a poor solvent for the polymer segments. In our studies, the Flory–Huggins interaction parameters ( $\chi$ ) for the polymer–solvent binaries are typically greater than 0.8.<sup>1–5</sup> Nonetheless, the experimental evidence to date suggests that solvent screening promotes miscibility and is the dominant influence of compressible fluid sorption in UCST-type systems. Second, hydrostatic pressure effects on the phase behavior of blends and block copolymers<sup>11–17</sup> are inherently coupled to the use of compressed solvents. In all cases studied to date, however, the hydrostatic contribution is secondary to solvent effects at modest pressures.<sup>1,2,4</sup> Finally, the sorption of a compressed diluent can lead to an increase in isothermal compressibility relative to the neat melt.<sup>1,18</sup> Fluid sorption can, therefore, add entropic contributions to phase instability related to increases in component compressibility that are negligible in liquid-solvent systems. The effect of these contributions would be most pronounced for systems exhibiting LDOT- or LCST-type behavior but may be less important for systems exhibiting UCST-type behavior. These trends are apparent in the data: fluid sorption destabilizes LCST and LDOT systems, causing dramatic reductions in phase-separation temperatures, but the same effect is not apparent in ODT systems. The differences in LDOT and ODT behavior persist even in systems

that are chemically similar, such as the styrene/*n*-alkyl methacrylate copolymers described previously.<sup>5</sup>

Although compressibility appears to be at the heart of sorption-induced phase segregation in fluid/polymer systems, it is of course difficult to isolate enthalpic and entropic contributions to phase equilibrium experimentally for any one system. Alternatively, one can attempt to isolate these contributions in an approximate manner through experimental design. Our previous studies involving a series of light alkane solvents in LCST and UCST systems and CO<sub>2</sub> sorption in poly(styrene-*b*-*n*-alkyl methacrylate) copolymers exhibiting ODT and LDOT behavior were conducted in this vein. Here we take another approach and study a system in which enthalpic interactions contribute very little to the underlying phase behavior of the binary mixture. Further, we choose a compressible fluid (CO<sub>2</sub>) that is a poor solvent for both polymers and exhibits essentially neutral selectivity for the blend components. Consequently, all enthalpic interactions in the ternary system are quite weak. Specifically, we selected a mixture of deuterated polybutadiene (d-PBD) and polyisoprene (PI), a blend that is reported to be nearly ideal with respect to interchain enthalpic interactions. Each component is in effect a random copolymer that possesses a distribution of chains containing 1,2-, 1,4-, and 3,4-linkages in various proportions. These polydienes exhibit only the weak van der Waals interactions between the polymer segments. In the absence of specific interactions, the structures of these chains alone dictate the blend phase behavior.

We determined the phase behavior of the binary d-PBD/PI and ternary d-PBD/PI/CO<sub>2</sub> systems with small-angle neutron scattering (SANS). Temperature-dependent  $\chi$  values for d-PBD and PI are calculated from the binary SANS data and compared to previous results from the literature. CO<sub>2</sub> sorption in d-PBD thin films is measured with *in situ* high-pressure neutron reflectivity. Sorption isotherms for PI are calculated with experimental data from the literature and the Sanchez–Lacombe EOS. Finally, CO<sub>2</sub>/polymer interaction parameters are calculated from the data with Flory’s activity equation.

## EXPERIMENTAL

Protonated PI and d-PBD were purchased from Polymer Source (Dorval, PQ Canada). PI had a

**Table 1.** Polymer Characteristics

Polymer	Molecular Weight (kg/mol)	PDI	1,4-Addition	1,2-Addition	3,4-Addition
d-PBD	140	1.08	82%	18%	—
PI	84.2	1.03	96%	—	4%

total number-average molecular weight ( $M_n$ ) of 84,200 g/mol, a polydispersity index (PDI) of 1.03, and isomer contents of 81 mol % cis 1,4-addition, 15 mol % trans 1,4-addition, and 4 mol % 3,4-addition. d-PBD had a total  $M_n$  value of 140,000 g/mol, a PDI of 1.08, and isomer contents of 82 mol % 1,4-addition and 18 mol % 1,2-addition (Table 1). The glass-transition temperatures of the polymers, as determined with a DuPont differential scanning calorimetry (DSC) instrument, were  $-70$  °C for PI and  $-90$  °C for d-PBD.

Samples for SANS experiments were prepared by the dissolution of appropriate amounts of PI and d-PBD in toluene to form a 5–7 wt % polymer solution. The toluene was then slowly evaporated at room temperature for more than 10 h and then for at least 3 days *in vacuo* at room temperature. The polymer blends were pressed into aluminum rings (1 mm thick  $\times$  6.4 mm in diameter) at room temperature. Air trapped inside the pressed polymer blends was carefully removed, and the resultant samples were stored *in vacuo* at room temperature until transferred to the high-pressure cell. Details of the cell are provided elsewhere.<sup>2</sup> CO<sub>2</sub> (Coleman-grade, 99.99%) was purchased from Merriam Graves and used as received. A computer-controlled high-pressure pump (ISCO, Inc.) was used to deliver CO<sub>2</sub> at elevated pressures.

SANS experiments were conducted with the NG7 30-m instrument at the Cold Neutron Research Facility of the National Institute of Standards and Technology (NIST; Gaithersburg, MD). All samples were purged with low-pressure CO<sub>2</sub> before data collection. The configuration of the instrument for all data presented here is as follows: wavelength ( $\lambda$ ) = 7.0 Å,  $\Delta\lambda/\lambda$  = 0.11, sample-to-detector distance = 350 cm, beam diameter = 4.40 cm, and beam-stop diameter = 5.08 cm. Scattering profiles were taken *in situ* in the presence of CO<sub>2</sub> at constant densities as a function of temperature (from 0.10 to 0.40 g/cm<sup>3</sup>) or under isothermal conditions as a function of increasing CO<sub>2</sub> density. The two-dimensional raw data were corrected for background scattering at appropriate densities of CO<sub>2</sub> and detector sensitivity, scaled to absolute units (cm<sup>-1</sup>) with a SiO<sub>2</sub> stan-

dard, and finally radially averaged. The location of the LCST at the ambient pressure was obtained with plots of the reciprocal intensity at a wavevector of  $\mathbf{q} = 0$  (obtained by extrapolation with the NIST data-reduction software) versus the inverse absolute temperature.<sup>19</sup> For samples containing CO<sub>2</sub>, the location of the LCST was determined in the same manner. At temperatures (or pressures) above the LCST, the extrapolated scattering intensity at  $\mathbf{q} = 0$  was infinite, providing direct confirmation of an upper bound on the location of the LCST in the presence of CO<sub>2</sub>.

The d-PBD film for the *in situ* reflectivity measurements was prepared via spin coating from a 2.5 wt % solution in toluene onto a polished single-crystal quartz. The initial film thickness was 961 Å. The thickness of the film swollen by CO<sub>2</sub> at various pressures was obtained from theoretical fits to the experimental neutron reflectivity profiles as a function of  $\mathbf{q}$  with a bilayer model. The experiments were performed on the NG7 reflectometer with a horizontal geometry at the Cold Neutron Source of NIST. Details of the measurement techniques and the high-pressure reflectivity cell are available elsewhere.<sup>20</sup>

### Phase Behavior of the Polybutadiene (PBD)/PI Binary Blends

There have been numerous studies of PBD/PI binary blends with various techniques, including SANS,<sup>21,22</sup> small-angle light scattering,<sup>22</sup> DSC,<sup>21,23–26</sup> NMR spectroscopy,<sup>25,27</sup> and dilatometry.<sup>21,23,24,27,28</sup> The 1,2-microstructure of PBD [poly(vinyl ethylene) (PVE)] is completely miscible with 1,4-PI, even at very high molecular weights. In contrast, a random copolymer of PBD (comprised of 1,2- and 1,4-microstructures), is partially miscible with 1,4-PI, resulting in an LCST-type behavior.<sup>21,23</sup> Because these mixtures have nearly ideal enthalpic interactions between the components, phase segregation cannot be attributed to weakening specific interactions with increases in system temperature. Rather, a series of studies suggest that phase segregation occurs because of an increasing disparity in the volumet-

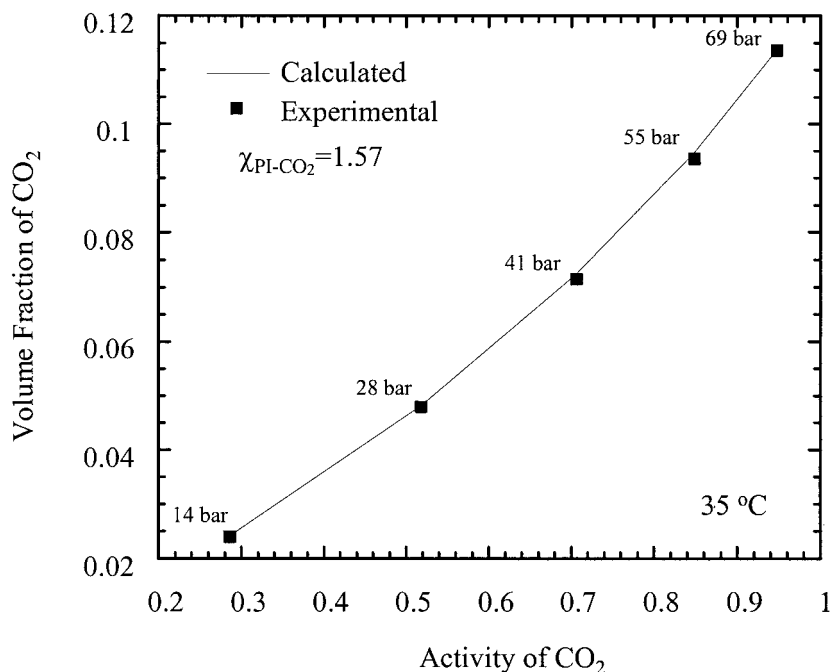


**Figure 1.** CO<sub>2</sub> sorption in PI at 35 °C. The solid line is a fit to the data with eq 1 and a  $\chi$  value of 1.57.

ric properties of the components upon heating, as evidenced by their thermal expansion coefficients and isothermal compressibilities.

Roland and Trask<sup>23</sup> found that PBD and PI exhibit a disparity in their thermal expansion coefficients, which imparts a small but significant contribution to the demixing of the blend. This is manifest in a volume contraction upon mixing and can influence both the enthalpy and entropy of mixing. Akiyama and coworkers<sup>27,28</sup> found a measurable discontinuity in the thermal expansion coefficients of a blend of PBD and PI below and above its LCST. Moreover, they reported a negative deviation in the volume change upon mixing at a temperature below the LCST and a positive deviation above the LCST and found the volume of the mixture to be additive at the LCST.<sup>27</sup> In contrast, the thermal expansion coefficients of PVE and PI, which are miscible at all molecular weights, are nearly the same at all conditions, and so the densities of blends of various compositions are additive (zero volume change upon mixing).<sup>23</sup> Akiyama and coworkers interpreted the experimental negative excess volume of mixing for PBD and PI in terms of the Flory EOS theory. The interaction parameter required to fit the negative excess mixing volume was shown to be influenced by the difference in the external degrees of freedom between the homopolymers and the mixture. This contribution, called the *structural effect*, can be represented in terms of characteristic temperatures.<sup>28</sup>

Finally, Hashimoto and coworkers studied the effects of the various microstructures of d-PBD and PI by SANS and interpreted the results with the copolymer blend theory of ten Brinke et al.<sup>22,29,30</sup> The effective binary interaction parameter per monomer unit ( $\chi_{\text{eff}}$ ) obtained could be cast in the  $A + B/T$  form typical of LCST-type systems. Variations in microstructures affected predominantly the temperature-independent entropic term rather than the temperature-dependent enthalpic term.

## RESULTS

### Interaction of CO<sub>2</sub> with d-PBD and PI

Knowledge of the interaction of CO<sub>2</sub> with the homopolymers is a prerequisite for interpreting the results for the ternary system. It is well known that CO<sub>2</sub> is generally a poor solvent for polymers. Notable exceptions include certain amorphous fluoropolymers, poly(dimethylsiloxane)s, and poly(ether carbonate)s.<sup>31</sup> The polymers used in this study are insoluble under the conditions studied, and so our experimental system consists of a pure CO<sub>2</sub> fluid phase in contact with the CO<sub>2</sub>-diluted polymer phase(s). The sorption isotherm of CO<sub>2</sub> in 1,4-PI at 35 °C is shown in Figure 1.<sup>32</sup> The solubility of CO<sub>2</sub> in the polymer is modest: at densities of 0.1 and 0.2 g/cm<sup>3</sup> CO<sub>2</sub>, the

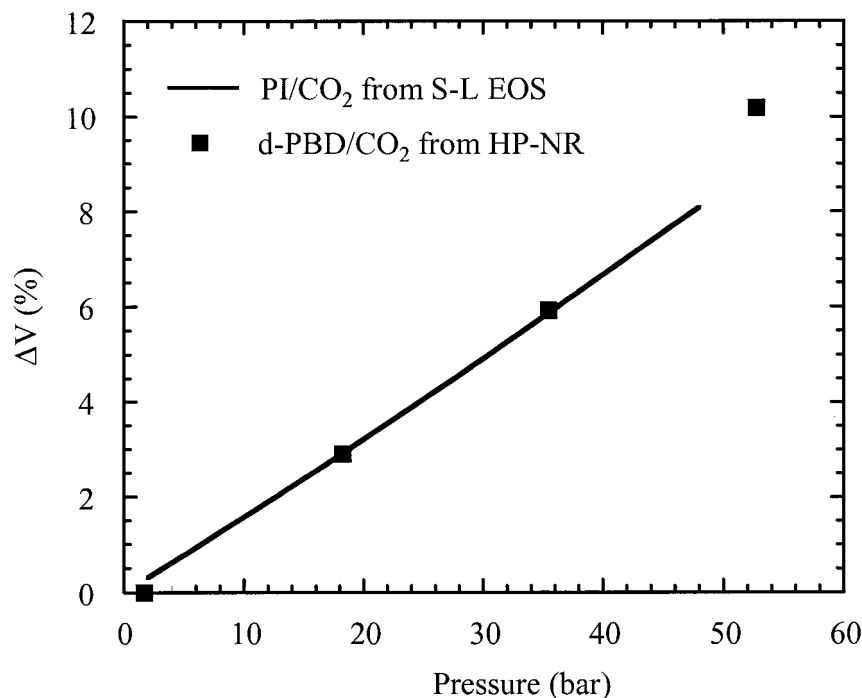


**Figure 2.** Swelling of CO<sub>2</sub> in d-PBD and PI at 40 °C. The swelling of d-PBD was measured with *in situ* high-pressure neutron reflectivity. The sorption in PI was calculated with the Sanchez–Lacombe EOS and a binary interaction parameter ( $\delta_{ij} = 0.046$ ) determined with an experimental absorption isotherm at 35 °C.<sup>32</sup>

concentration of CO<sub>2</sub> is approximately 7.5 and 10 vol %, respectively. Experimental data for the swelling of a 961-Å d-PBD film by the sorption of CO<sub>2</sub> at 40 °C, as determined by neutron reflectivity, is shown in Figure 2. Also shown in the figure are points along the PI/CO<sub>2</sub> isotherm calculated with the Sanchez–Lacombe EOS with a binary interaction parameter calculated with the data in Figure 1. The pure component parameters in the Sanchez–Lacombe EOS formalism for PI, given in Table 2, were regressed by the fitting of polymer density data at various temperatures in the low-pressure range of 1–200 bar with a Levenberg–Marquardt least-squares algorithm.<sup>33–35</sup> The sorption isotherms for both polymers are essen-

**Table 2.** Characteristic Parameters Used in the Sanchez–Lacombe EOS To Evaluate the Swelling of PI by Sorbed CO<sub>2</sub><sup>a</sup>

Component	$P^*$ (atm)	$T^*$ (K)	$\rho^*$ (g/cm <sup>3</sup> )
PI	3976	682	0.938
CO <sub>2</sub> <sup>21</sup>	5670	305	1.510

<sup>a</sup>  $P^*$  is the characteristic pressure,  $T^*$  is the characteristic temperature, and  $\rho^*$  is the characteristic density.

tially superimposed. This result is not surprising, given the similarity of the chemical structures, and indicates CO<sub>2</sub> sorption selectivity is either very low or nonexistent.

The weak interaction between CO<sub>2</sub> and nonpolar polymers is evident from an evaluation of  $\chi$ , which can be obtained with sorption data and Flory’s activity equation:

$$\ln A_{\text{CO}_2} = \ln(1 - \phi_{\text{poly}}) + \left(1 - \frac{r_{\text{CO}_2}}{r_{\text{poly}}}\right)\phi_{\text{poly}} + \chi\phi_{\text{poly}}^2 \quad (1)$$

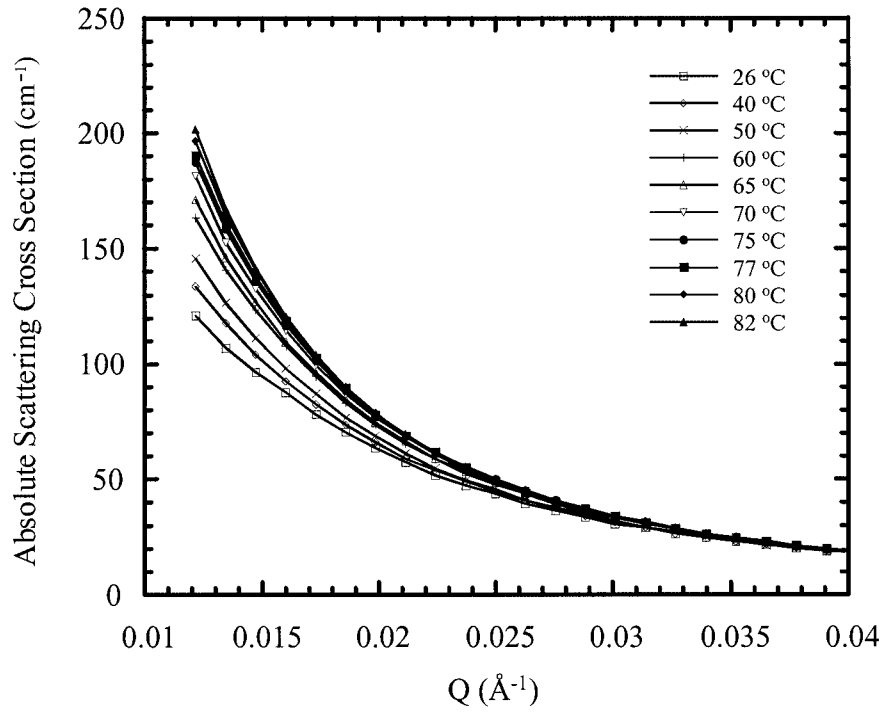
where  $A$  is the activity of CO<sub>2</sub> evaluated with the Peng–Robinson EOS,  $r$  is a size parameter, and  $\phi_i$  is the volume fraction of component  $i$ . A fit of the sorption data, as shown in Figure 1, yields  $\chi = 1.57$  for 1,4-PI/CO<sub>2</sub> and  $\chi = 1.49$  d-PBD/CO<sub>2</sub>. This difference is not significant within experimental error.

## Phase Behavior Determination by SANS

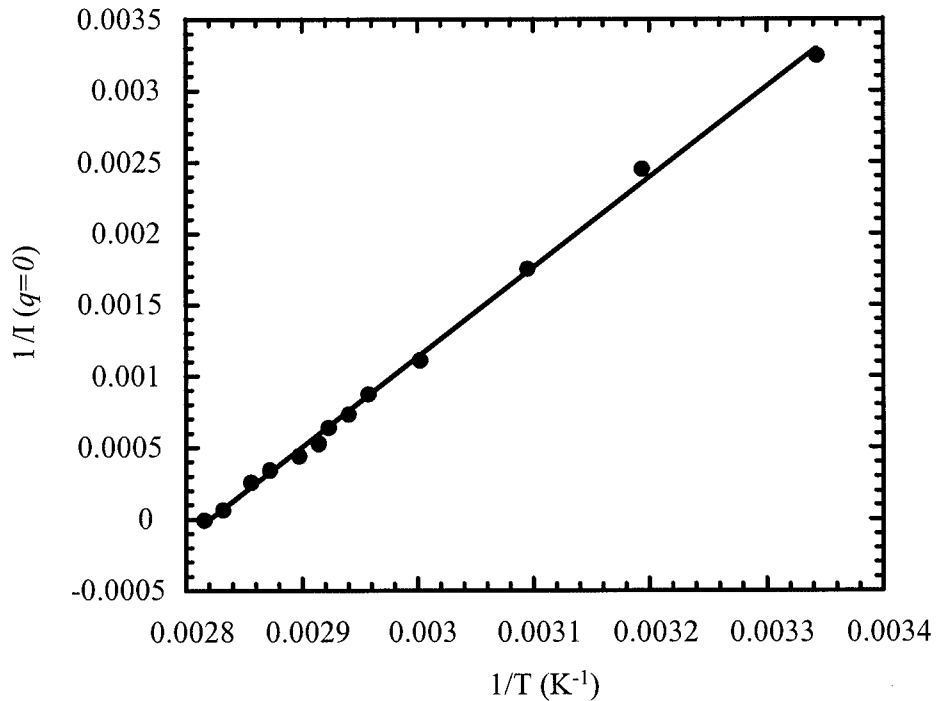
### Binary Blends

SANS results indicate that the binary d-PBD/PI blends chosen for this study exhibit molecular-





(a)



(b)

**Figure 3.** (a) SANS profiles of a 50/50 d-PBD/PI blend as a function of temperature and (b) the LCST determination of a 50/50 d-PBD/PI blend with a plot of  $1/I(q=0)$  extrapolated versus  $1/T$ .

weight-dependent LCST-type behavior, as anticipated from their respective microstructures.<sup>22,29</sup> Figure 3(a,b) shows typical SANS profiles for a

50/50 d-PBD/PI blend and the estimation of the spinodal LCST, respectively. The transition temperature obtained is intermediate between the

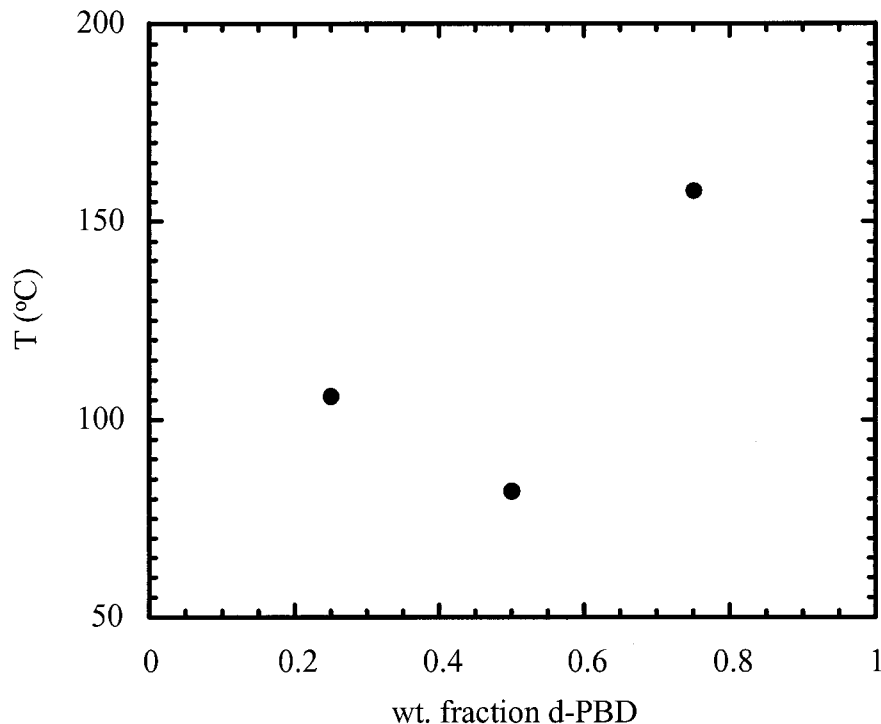


**Figure 4.** LCST curve for d-PBD/PI blends determined by SANS.

spinodal and binodal curves because of the heating rates used in this study. Nevertheless, the linear dependence of  $1/I(\mathbf{q} = 0)$  with  $1/T$  indicates that the estimated phase-separation temperature is closer to the spinodal temperature. The resulting LCST curve (Fig. 4) for the thermal transitions is more symmetric with respect to the blend composition than those for other mixtures such as PS and PVME. This can be partly ascribed to the significantly lower compositional dependence of the volume change upon the mixing of d-PBD and PI.

$\chi$  between the polymers in the homogeneous blend can be calculated from the SANS data with an incompressible random phase approximation (RPA) formalism for asymmetric polymers.<sup>29</sup>

$$\frac{k_N}{S(\mathbf{q})} = \frac{1}{\phi_1 z_{n1} v_1 S_1(\mathbf{q})} + \frac{1}{\phi_2 z_{n2} v_2 S_2(\mathbf{q})} - \frac{2\chi}{v_0} \quad (2)$$

where

$$k_N = N_A \left( \frac{a_1}{v_1} - \frac{a_2}{v_2} \right) \quad (3)$$

$$S_i(\mathbf{q}) = \left( \frac{2}{x_i^2} \right) \left[ x_i - 1 + \left( \frac{h_i}{h_i + x_i} \right)^{h_i} \right] \quad (4)$$

$$x_i = \mathbf{q}^2 \langle R_0^2 \rangle = \frac{\mathbf{q}^2 z_{ni} b_i^2}{6} \quad (5)$$

$$h_i = \left( \frac{M_w}{M_n} \right)_i - 1 \quad (i = 1 \text{ or } 2) \quad (6)$$

where subscripts 1 and 2 denote the various quantities for the two components,  $a_i$  is the scattering length per mole of monomer units for neutrons ( $3.37 \times 10^{-13}$  cm/mol for PI and  $6.66 \times 10^{-12}$  cm/mol for d-PBD),  $v_i$  is the molar volume ( $75.6$  cm<sup>3</sup>/mol for PI and  $60.4$  cm<sup>3</sup>/mol for d-PBD),  $z_{ni}$  is the number-average degree of polymerization (1239 for PI and 2333 for d-PBD),  $b_i$  is the statistical segment length,  $N_A$  is Avogadro's number,  $v_0$  is the molar volume of the reference cell, and  $S_i(\mathbf{q})$  is the Debye function for the  $i$ th component. Incoherent scattering was assumed to be negligible here, and  $b_{\text{d-PBD}}/b_{\text{PI}}$  was fixed to be unity, each given a value of  $7 \text{ \AA}$ .<sup>7</sup> Furthermore,  $v_0$  was calculated with the following equation:

$$v_0 = \left( \frac{\phi_1}{v_1} + \frac{\phi_2}{v_2} \right)^{-1} \quad (7)$$

A typical fit of the SANS curve for the 50/50 d-PBD/PI blend at  $40^\circ \text{C}$  is shown in Figure 5. Figure 6 shows the values of the interaction pa-

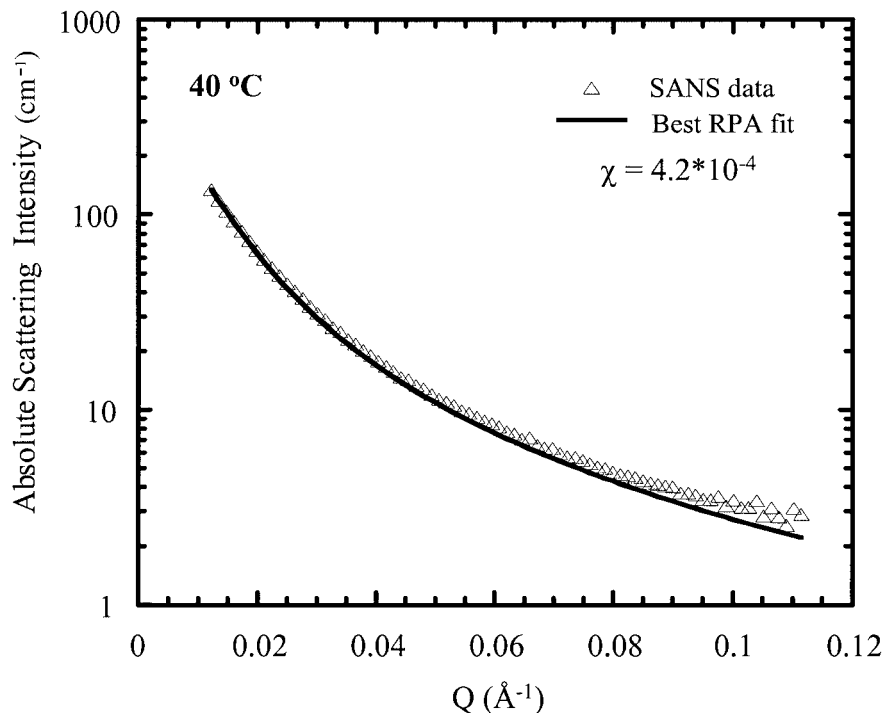


**Figure 5.** Typical RPA fit for  $\chi$  determination with SANS data for a 50/50 d-PBD/PI blend at 40 °C.

rameters for the different blends as a function of the temperature. An increase in the interaction parameter with increasing  $T$  is a signature of an LCST system, and the values of  $\chi_{\text{eff}}$ 's are consistent with the microstructure contents of the polymers.<sup>29</sup> It is important to note that the spinodal Flory–Huggins interaction parameter ( $\chi_s$ ) can be estimated as follows:

$$\chi_s = \frac{v_0}{2} \left( \frac{1}{\phi_1 z_{w1} v_1} + \frac{1}{\phi_2 z_{w2} v_2} \right) \quad (8)$$

where  $z_{wi}$  is the weight-average degree of polymerization.  $\chi_s$ , calculated with eq 8, is  $1.49 \times 10^{-3}$  for  $\phi_{\text{d-PBD}} = 0.232$ ,  $1.13 \times 10^{-3}$  for  $\phi_{\text{d-PBD}} = 0.475$ , and  $1.52 \times 10^{-3}$  for  $\phi_{\text{d-PBD}} = 0.731$ . The values obtained with eq 8 are slightly higher than the corresponding values obtained from the RPA. This may reflect the effect of the temperature schedule on these experiments. For our purpose, we maintain the same heating rates for the binary blend and the ternary system.

#### **d-PBD/PI/CO<sub>2</sub> System**

The neutron scattering intensity from a ternary mixture is a complicated function of both the intrinsic thermodynamics of the system and the contrast between the various binaries.<sup>19,36</sup> Here

we consider the effects of CO<sub>2</sub> sorption on contrast in d-PBD/PI/CO<sub>2</sub> mixtures. In SANS, the contrast factor between each binary is the square of the difference in the neutron scattering length densities. The scattering length densities of the three components in the ternary system are given in Table 3. Here, the density of CO<sub>2</sub> in the polymeric phase is assumed to be 0.97 g/cm<sup>3</sup>, regardless of its pressure in the vapor phase.<sup>37</sup> The evaluated  $[(b/v)_i - (b/v)_j]^2$  values show that there is a net decrease in the contrast between the dilated polymer phases in the system upon the addition of CO<sub>2</sub>. Therefore, any increase in the scattering of the system is due to increased concentration fluctuations between the polymer components.

SANS data for the ternary d-PBD/PI/CO<sub>2</sub> mixtures were obtained in a high-pressure cell. Increasing the degree of CO<sub>2</sub> sorption in the blends through pressure-mediated adjustments of the density in the vapor phase increased the scattering cross sections at 50 and 70 °C, well below their normal LCSTs, and ultimately resulted in phase separation for the 25/75 and 50/50 blends. Experiments were also conducted at constant densities of CO<sub>2</sub> at various temperatures. The approximate location of the depressed LCST, the temperature at which the blend separated completely in the presence of CO<sub>2</sub>, was determined as the point at



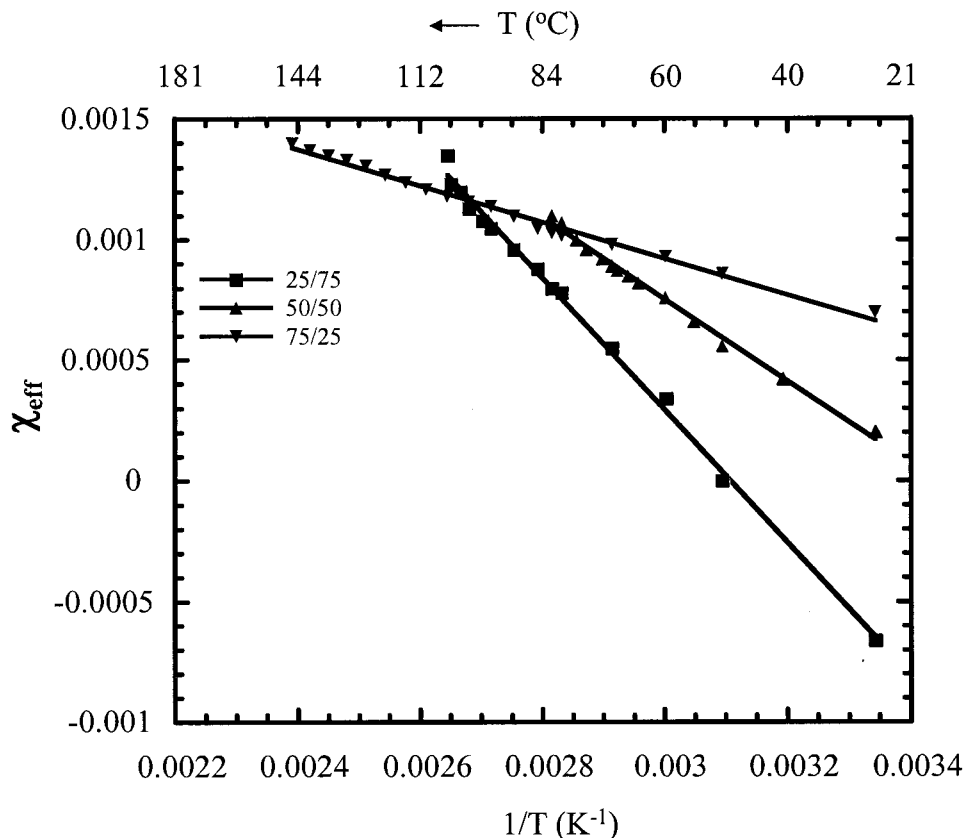


**Figure 6.**  $\chi_{\text{eff}}$  for homogeneous d-PBD/PI blends of various compositions with incompressible RPA (see the text for a discussion).

which the extrapolated intensities at  $q = 0$  became infinite. Figures 7 and 8 show the SANS results for a 50/50 d-PBD/PI blend at a constant  $\text{CO}_2$  density of  $0.2 \text{ g/cm}^3$  and the identification of the LCST from the extrapolated intensity at  $q = 0$ , respectively. It is important to note the linearity of  $1/I(q = 0)$  against  $1/T$  for the ternary blend, which reflects the weak enthalpic interactions with either polymer<sup>36,38</sup> and the small effect of  $\text{CO}_2$  on the contrast terms. The results of the study are presented in Table 4 with a continuous depression in the LCST of 25/75 and 50/50 blends with an increase in the  $\text{CO}_2$  pressure/density. The

data are not corrected for hydrostatic pressure effects that are inherent to the use of compressed solvents. It is well known that for LCST systems such as PS/PVME blends and P(S-*b*-nBMA) copolymers, the application of hydrostatic pressure opposes free-volume disparities between the components, which suppress phase separation and increase the LCST or LDOT.<sup>13,15,39</sup> Just as for the PS/PVME/ $\text{CO}_2$  and PS/PnBMA/ $\text{CO}_2$  systems, the effects of  $\text{CO}_2$  sorption dominate the effects of hydrostatic pressure, and the LCST decreases with increases in pressure and, therefore, solvent density.

**Table 3.** Neutron Scattering Length Densities (NSLDs) of d-PBD, PI, and  $\text{CO}_2$  and Contrast Factors for the Component Binaries

	d-PBD	PI	Dissolved $\text{CO}_2$
NSLD ( $10^{10} \text{ cm}^{-2}$ )	6.53	0.258	2.42
d-PBD contrast ( $10^{20} \text{ cm}^{-4}$ )	—	39.34	16.89
PI contrast ( $10^{20} \text{ cm}^{-4}$ )	39.34	—	4.67
Dissolved $\text{CO}_2$ contrast ( $10^{20} \text{ cm}^{-4}$ )	16.89	4.67	—

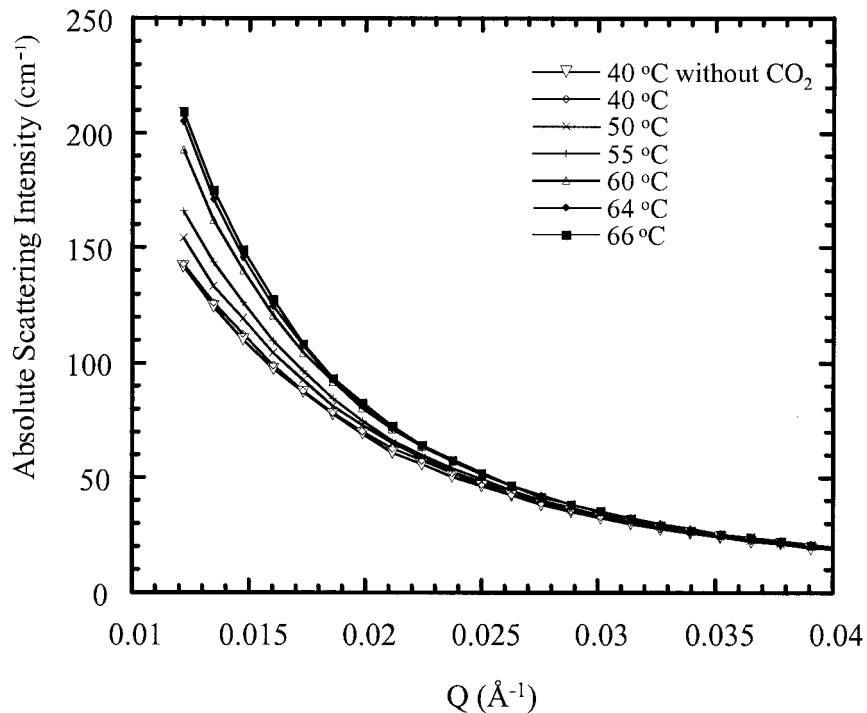


**Figure 7.** Isoplethic SANS profile (density of  $\text{CO}_2 = 0.2 \text{ g/cm}^3$ ) of a 50/50 d-PBD/PI blend as a function of temperature.

## DISCUSSION

A quantitative evaluation of the observed effect of  $\text{CO}_2$  sorption on the phase behavior of d-PBD/PI

blends is very difficult because the details of the chain microstructure and packing that give rise to LCST behavior in the underlying binary system are quite subtle and are difficult to capture accu-

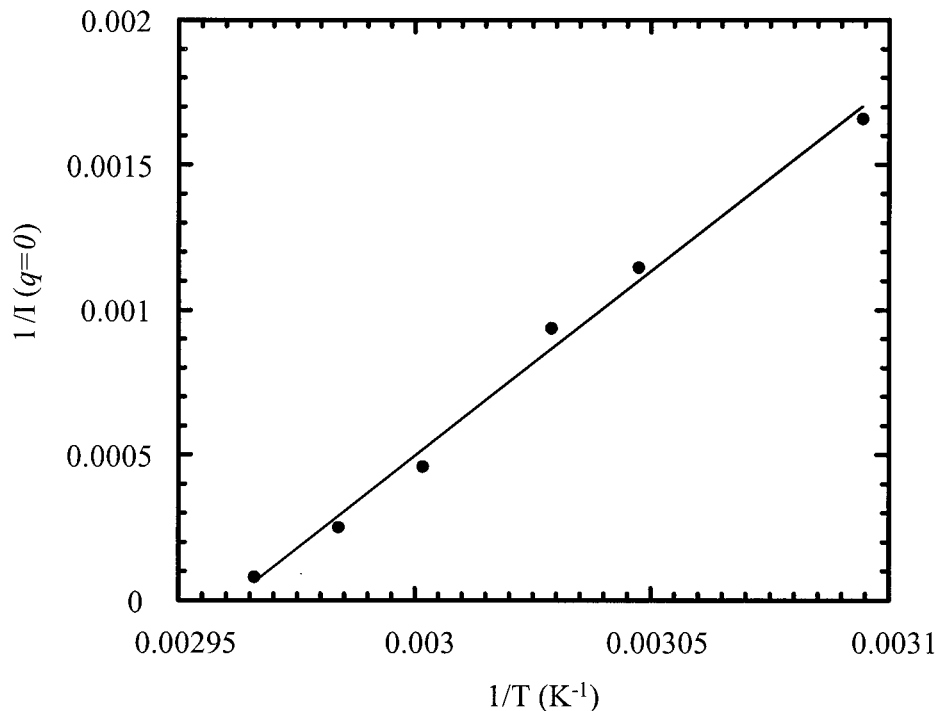


**Figure 8.** LCST determination for a 50/50 d-PBD/PI blend in the presence of  $\text{CO}_2$  at a density of  $0.2 \text{ g/cm}^3$  with the reciprocal of extrapolated scattering at  $\mathbf{q} = 0$  versus  $1/T$ .

**Table 4.** Binary d-PBD/PI LCSTs and Solvent-Induced Transitions at Various Densities of CO<sub>2</sub>

Composition	Constant Density:			
	Ambient Temperature (°C)	Temperature at 0.1 g/cm <sup>3</sup> (°C)	Temperature at 0.2 g/cm <sup>3</sup> (°C)	Temperature at 0.4 g/cm <sup>3</sup> (°C)
25/75	106	99	92	86
50/50	82	72	66	62

Composition	Isothermal CO <sub>2</sub> Pressurization		
	Ambient Temperature (°C)	Density at 70 °C	Density at 90 °C
25/75	106	– <sup>a</sup>	0.28 g/cm <sup>3</sup>
50/50	82	0.14 g/cm <sup>3</sup>	<sup>b</sup>

<sup>a</sup> The intensity increased, but the extrapolated  $1/I(\mathbf{q} = 0)$  term did not reach zero.

<sup>b</sup> Not run.

rately with an EOS. Moreover, recent work has suggested a coupling between structural effects, including chain packing, and energetics that has not been captured by EOS approaches.<sup>40,41</sup> Nonetheless, a qualitative analysis of the origin of this behavior is possible on the basis of the known behavior of the d-PBD/PI binary system and by comparisons to other blend/CO<sub>2</sub> systems for which there is more detailed information.

In binary polymer systems, stability is dictated by enthalpic interactions and by both the net compressibility of the system and the free-volume disparity between the components.<sup>8,10</sup> As stated earlier, the PI/PBD binary blend system is devoid of specific interactions, and the available data suggest that phase segregation in these systems is due to increasing disparity in the volumetric properties of the components upon heating, as evidenced by their thermal expansion coefficients and isothermal compressibilities.

CO<sub>2</sub> is a poor, essentially nonselective diluent for PI and PBD, yet its sorption at modest volume fractions destabilizes the blend. Because the enthalpic interactions between the various components in the PI/PBD/CO<sub>2</sub> are quite weak and CO<sub>2</sub> sorption in the chemically indistinguishable polymers is virtually nonselective, we do not expect solvent screening to dominate phase behavior. Instead we look toward entropic contributions, namely EOS effects, to phase instability. Compressibility is central to this issue, and its influence on polymer phase behavior has recently received increased attention.<sup>7,8,11,13–15,42–47</sup> We re-

viewed this work in the context of phase segregation induced by compressible fluid sorption in earlier articles.<sup>1,3,4</sup>

The sorption of gases and supercritical fluids into a rubbery polymer can increase the compressibility of the dilated melt relative to the pure polymer.<sup>1,18</sup> In fact, at low and modest pressures, the isothermal compressibility of the dilated polymer is raised by increasing system pressure because of the increasing solubility of the diluent.<sup>8,18</sup> In this respect, isothermal dilation by CO<sub>2</sub> mimics an increase in temperature. For multicomponent polymer systems in which CO<sub>2</sub> sorption is selective, increasing the system pressure imparts a dilation disparity between the components. Thus, for blends and block copolymers, fluid sorption not only increases system compressibility but also can exacerbate free-volume disparities between the dilated components upon phase segregation. Both factors can destabilize the system. The effect of increasing the temperature on the phase behavior of 25/75 and 50/50 d-PBD/PI blends in the presence of CO<sub>2</sub> can also be visualized in this light. The thermal expansion coefficient of the absorbed CO<sub>2</sub> in rubbery polymers is reported to be a weak function of the chemical nature of the polymer and is approximately  $2 \times 10^{-3} \text{ }^\circ\text{C}^{-1}$ .<sup>48</sup> This value is similar to or rather larger than the disparity in the thermal expansion coefficients of PBD with 92% 1,4-units ( $1.8 \times 10^{-3} \text{ }^\circ\text{C}^{-1}$ ) and PI ( $0.93 \times 10^{-3} \text{ }^\circ\text{C}^{-1}$ ), which is the origin of immiscibility in the polymer blends.<sup>23</sup> Hence, the slightest disparity in the

sorption levels of CO<sub>2</sub> in PBD and PI would lead to an increase in the dilation disparity similar to an increase in temperature. Moreover, the presence of CO<sub>2</sub> adds free volume to the system by exacerbating the packing disparity of the polymers and, therefore, increasing the propensity of the polymers to phase-separate. This explanation is also consistent with the lower sensitivity of the 75/25 blend to phase segregation upon CO<sub>2</sub> sorption. The location of the transition in the 75/25 binary system is 160 °C. At this temperature, pressures required to achieve significant CO<sub>2</sub> solubility are quite high, and the hydrostatic pressure effect may compete with the effects of dilation. We also note that the temperature dependence of  $\chi$  in the 75/25 blend is much weaker than that of 50/50 and 25/75 blends. If disparities in the volumetric properties are responsible for the increase in  $\chi$ , as suggested by the available data, this blend is less susceptible to thermal dilation, which is aggravated by CO<sub>2</sub> sorption.

We note that the solvent-induced depression of the LCST in the d-PBD/PI blend is considerably smaller than that observed in the PS/PVME and PS/PnBMA systems. This is likely attributable to the exceeding weak selectivity of CO<sub>2</sub> in the d-PBD/PI system. In the case of PS/PVME, PVME absorbs significantly more CO<sub>2</sub> than PS, and this aggravates the existing disparity in compressibility and thermal expansion coefficients. Consequently, the volume change on the mixing of the dilated components would be larger than that of the homopolymers, and CO<sub>2</sub> sorption destabilizes the system. In the case of PS/PnBMA systems, CO<sub>2</sub> sorption is highly selective for PnBMA because of the favorable interactions between the quadrupole moment of CO<sub>2</sub> and the dipole of the carbonyl group of PnBMA.<sup>4</sup> Depressions of the LDOT in P(*S-b*-nBMA) upon CO<sub>2</sub> sorption can exceed 250 °C. In both the PS/PVME and PS/PnBMA systems, CO<sub>2</sub> is selective for the component with the greater intrinsic compressibility. We have now begun work on systems in which the fluid is selective for the component that is less compressible.

## CONCLUSIONS

The sorption of CO<sub>2</sub> in nearly ideal d-PBD/PI blends induces phase segregation at modest solvent loadings. All enthalpic interactions in this ternary system are weak. CO<sub>2</sub> is a poor, virtually nonselective solvent for the polymers, and the polydienes exhibit only weak van der Waals in-

teractions between the polymer segments. Thus, phase separation due to solvent screening is unlikely. Although definitive conclusions cannot be drawn on the basis of these data alone, it is likely that CO<sub>2</sub> sorption aggravates the disparity in the volumetric properties of the blend components that induces LCST behavior in d-PBD/PI binary blends. This result is consistent with solvent-induced segregation in the PS/PVME/CO<sub>2</sub> and PS/PnBMA/CO<sub>2</sub> systems, which exhibit strong and weak polymer–polymer interactions, respectively, although the depth of the depression is smaller because of the nearly nonselective sorption of CO<sub>2</sub> in the d-PBD/PI system.

This work was supported by the Material Research Science and Engineering Center at the University of Massachusetts, the David and Lucile Packard Foundation, and the Camille Dreyfus Teacher–Scholar program. B. D. Vogt acknowledges support from the NSF Graduate Research Fellowship program. The Cold Neutron Research Facility is supported by NIST and NSF under agreement number DMR-9423101. The authors thank Boualem Hammouda (NIST) for helpful discussions.

## REFERENCES AND NOTES

1. RamachandraRao, V. S.; Watkins, J. J. *Macromolecules* 2000, 33, 5143–5152.
2. Vogt, B. D.; Brown, G. D.; RamachandraRao, V. S.; Watkins, J. J. *Macromolecules* 1999, 32, 7907–7912.
3. Vogt, B. D.; Watkins, J. J. *Macromolecules* 2002, 35, 4056–4063.
4. Watkins, J. J.; Brown, G. D.; RamachandraRao, V. S.; Pollard, M. A.; Russell, T. P. *Macromolecules* 1999, 32, 7737–7740.
5. Vogt, B. D.; RamachandraRao, V. S.; Gupta, R. R.; Lavery, K. A.; Francis, T. J.; Russell, T. P.; Watkins, J. J. *Macromolecules* 2003, 36, 4029–4036.
6. Walker, T. A.; Raghavan, S. R.; Royer, J. R.; Smith, S. D.; Wignall, G. D.; Melnichenko, Y.; Khan, S. A.; Spontak, R. J. *J Phys Chem B* 1999, 103, 5472–5476.
7. Cho, J. *Macromolecules* 2000, 33, 2228–2241.
8. Hino, T.; Prausnitz, J. M. *Macromolecules* 1998, 31, 2636–2648.
9. Patterson, D.; Robard, A. *Macromolecules* 1978, 11, 690.
10. Sanchez, I. C. In *Polymer Compatibility and Incompatibility: Principles and Practices*; Solc, K., Ed.; Harwood: Chur, Switzerland, 1982; Vol. 2, p 59.
11. Pollard, M.; Russell, T. P.; Ruzette, A. V.; Mayes, A. M.; Gallot, Y. *Macromolecules* 1998, 31, 6493–6498.

12. Hajduk, D. A.; Gruner, S. M.; Erramilli, S.; Register, R. A.; Fetters, L. J. *Macromolecules* 1996, 29, 1473–1481.
13. Hammouda, B.; Bauer, B. J. *Macromolecules* 1995, 28, 4505–4508.
14. Hammouda, B.; Lin, C. C.; Balsara, N. P. *Macromolecules* 1995, 28, 4765–4767.
15. Janssen, S.; Schwahn, D.; Mortensen, K.; Springer, T. *Macromolecules* 1993, 26, 5587–5591.
16. Schwahn, D.; Frielinghaus, H.; Mortensen, K.; Almdal, K. *Phys B* 1998, 241, 1029–1031.
17. Steinhoff, B.; Rullmann, M.; Wenzel, M.; Junker, M.; Alig, I.; Oser, R.; Stuhn, B.; Meier, G.; Diat, O.; Bosecke, P.; Stanley, H. B. *Macromolecules* 1998, 31, 36–40.
18. Garg, A.; Gulari, E.; Manke, C. W. *Macromolecules* 1994, 27, 5643–5653.
19. Higgins, J. S.; Benoit, H. *Polymers and Neutron Scattering*; Clarendon: Oxford, 1994.
20. Gupta, R. R.; Lavery, K. A.; Francis, T. J.; Webster, J. R. P.; Smith, G. S.; Russell, T. P.; Watkins, J. J. *Macromolecules* 2003, 36, 346–352.
21. Trask, C. A.; Roland, C. M. *Polym Commun* 1988, 29, 332–334.
22. Hasegawa, H.; Sakurai, S.; Takenaka, M.; Hashimoto, T.; Han, C. C. *Macromolecules* 1991, 24, 1813–1819.
23. Roland, C. M.; Trask, C. A. *Rubber Chem Technol* 1988, 62, 896.
24. Massie, J. M.; Halasa, A. F.; Thudium, R. N.; Burkhart, C. W. *ANTEC* 1992, 2, 1043.
25. Bahani, M.; Laupretre, F.; Monnerie, L. *J Polym Sci Part B: Polym Phys* 1995, 33, 167–178.
26. Kawahara, S.; Akiyama, S.; Ueda, A. *Polym J* 1989, 21, 221–229.
27. Kawahara, S.; Akiyama, S. *Polym J* 1991, 23, 7–14.
28. Kawahara, S.; Sato, K.; Akiyama, S. *J Polym Sci Part B: Polym Phys* 1994, 32, 15–20.
29. Sakurai, S.; Jinnai, H.; Hasegawa, H.; Hashimoto, T.; Han, C. C. *Macromolecules* 1991, 24, 4839–4843.
30. ten Brinke, G.; Karasz, F. E.; MacKnight, W. M. *Macromolecules* 1983, 16, 1827–1832.
31. Sarbu, T.; Styranec, T.; Beckman, E. J. *Nature* 2000, 405, 165–168.
32. Zhang, Y.; Gangwani, K. K.; Lemert, R. M. *J Supercrit Fluids* 1997, 11, 115–134.
33. Yi, Y. X.; Zoller, P. *J Polym Sci Part B: Polym Phys* 1993, 31, 779–788.
34. Sanchez, I. C. *Polym Lett Ed* 1977, 15, 71.
35. Pottiger, M. T.; Laurence, R. L. *J Polym Sci Polym Phys Ed* 1984, 22, 903–907.
36. Hammouda, B. *Adv Polym Sci* 1993, 106, 87–133.
37. Fleming, G. K.; Koros, W. J. *Macromolecules* 1986, 19, 2285–2291.
38. Ijichi, Y.; Hashimoto, T. *Polym Commun* 1988, 29, 135–138.
39. Pollard, M.; Russell, T. P.; Ruzette, A. V.; Mayes, A. M.; Gallot, Y. *Macromolecules* 1998, 31, 6493–6498.
40. Almdal, K.; Hillmyer, M. A.; Bates, F. S. *Macromolecules* 2002, 35, 7685–7691.
41. Kumar, S. K.; Weinhold, J. D. *Phys Rev Lett* 1996, 77, 1512–1515.
42. Kumar, S. K.; Veytsman, B. A.; Maranas, J. K.; Crist, B. *Phys Rev Lett* 1997, 79, 2265–2268.
43. Cho, J. *Macromolecules* 2001, 34, 6097.
44. Dudowicz, J.; Freed, K. F. *Macromolecules* 1995, 28, 6625–6641.
45. Dudowicz, J.; Freed, K. F. *Macromolecules* 1995, 28, 6625–6641.
46. Rabeony, M.; Lohse, D. J.; Garner, R. T.; Han, S. J.; Graessley, W. W.; Migler, K. B. *Macromolecules* 1998, 31, 6511–6514.
47. Krishnamoorti, R.; Graessley, W. W.; Dee, G. T.; Walsh, D. J.; Fetters, L. J.; Lohse, D. J. *Macromolecules* 1996, 29, 367–376.
48. Kamiya, Y.; Naito, Y.; Mizoguchi, K. *J Polym Sci Part B: Polym Phys* 1989, 27, 2243–2250.